

Search for the in-situ production of ^{77}Ge in the GERDA neutrinoless double-beta decay experiment

The GERDA collaboration^a,

M. Agostini¹⁰, A. Alexander¹⁰, G. Araujo²¹, A.M. Bakalyarov¹⁵,
M. Balata¹, I. Barabanov^{13,b}, L. Baudis²¹, C. Bauer⁹, S. Belogurov^{14,13,c},
A. Bettini^{18,19}, L. Bezrukov¹³, V. Biancacci³, E. Bossio¹⁷, V. Bothe⁹,
R. Brugnera^{18,19}, A. Caldwell¹⁶, S. Calgato^{18,19}, C. Cattadori¹¹,
A. Chernogorov^{14,15}, P.-J. Chiu²¹, T. Comellato¹⁷, V. D'Andrea³,
E.V. Demidova¹⁴, N. Di Marco², E. Doroshkevich¹³, M. Fomina⁷,
A. Gangapshev^{13,9}, A. Garfagnini^{18,19}, C. Gooch¹⁶, P. Grabmayr²⁰,
V. Gurentsov¹³, K. Gusev^{7,15,17}, J. Hakenmüller^{9,d}, S. Hemmer¹⁹,
W. Hofmann⁹, J. Huang²¹, M. Hult⁸, L.V. Inzhechik^{13,e}, J. Janicskó
Csáthy^{17,f}, J. Jochum²⁰, M. Junker¹, V. Kazalov¹³, Y. Kermaïdic⁹,
H. Khushbakht²⁰, T. Kihm⁹, K. Kilgus²⁰, I.V. Kirpichnikov¹⁴,
A. Klimenko^{9,7,g}, K.T. Knöpfle⁹, O. Kochetov⁷, V.N. Kornoukhov^{13,c},
P. Krause¹⁷, V.V. Kuzminov¹³, M. Laubenstein¹, M. Lindner⁹, I. Lippi¹⁹,
A. Lubashevskiy⁷, B. Lubsandorzhiev¹³, G. Lutter⁸, C. Macolino³,
B. Majorovits¹⁶, W. Maneschg⁹, G. Marshall¹⁰, M. Misiaszek⁵, M. Morella²,
Y. Müller²¹, I. Nemchenok^{7,g}, M. Neuberger¹⁷, L. Pandola⁴, K. Pelczar⁸,
L. Pertoldi^{17,19}, P. Piseri¹², A. Pullia¹², C. Ransom²¹, L. Rauscher²⁰,
M. Redchuk¹⁹, S. Riboldi¹², N. Rumyantseva^{15,7}, C. Sada^{18,19}, S. Sailer⁹,
F. Salamida³, S. Schönert¹⁷, J. Schreiner⁹, A.-K. Schütz^{20,h}, O. Schulz¹⁶,
M. Schwarz¹⁷, B. Schwingenheuer⁹, O. Selivanenko¹³, E. Shevchik⁷,
M. Shirchenko⁷, L. Shtembari¹⁶, H. Simgen⁹, A. Smolnikov^{9,7}, D. Stukov¹⁵,
S. Sullivan⁹, A.A. Vasenko¹⁴, A. Veresnikova¹³, C. Vignoli¹, K. von
Sturm^{18,19}, T. Wester⁶, C. Wiesinger¹⁷, M. Wojcik⁵, E. Yanovich¹³,
B. Zatschler⁶, I. Zhitnikov⁷, S.V. Zhukov¹⁵, D. Zinatulina⁷, A. Zschocke²⁰,
K. Zuber⁶, and G. Zuzel⁵.

¹ INFN Laboratori Nazionali del Gran Sasso, Assergi, Italy

² INFN Laboratori Nazionali del Gran Sasso and Gran Sasso Science Institute, Assergi, Italy

³ INFN Laboratori Nazionali del Gran Sasso and Università degli Studi dell'Aquila, L'Aquila, Italy

⁴ INFN Laboratori Nazionali del Sud, Catania, Italy

⁵ Institute of Physics, Jagiellonian University, Cracow, Poland

⁶ Institut für Kern- und Teilchenphysik, Technische Universität Dresden, Dresden, Germany

⁷ Joint Institute for Nuclear Research, Dubna, Russia

⁸ European Commission, JRC-Geel, Geel, Belgium

⁹ Max-Planck-Institut für Kernphysik, Heidelberg, Germany

¹⁰ Department of Physics and Astronomy, University College London, London, UK

¹¹ INFN Milano Bicocca, Milan, Italy

¹² Dipartimento di Fisica, Università degli Studi di Milano and INFN Milano, Milan, Italy

¹³ Institute for Nuclear Research of the Russian Academy of Sciences, Moscow, Russia

¹⁴ Institute for Theoretical and Experimental Physics, NRC "Kurchatov Institute", Moscow, Russia

¹⁵ National Research Centre "Kurchatov Institute", Moscow, Russia

¹⁶ Max-Planck-Institut für Physik, Munich, Germany

¹⁷ Physik Department, Technische Universität München, Germany

¹⁸ Dipartimento di Fisica e Astronomia, Università degli Studi di Padova, Padua, Italy

¹⁹ INFN Padova, Padua, Italy

²⁰ Physikalisches Institut, Eberhard Karls Universität Tübingen, Tübingen, Germany

²¹ Physik-Institut, Universität Zürich, Zurich, Switzerland

Received: date / Accepted: date

Abstract The beta decay of ^{77}Ge and $^{77\text{m}}\text{Ge}$, both produced by neutron capture on ^{76}Ge , is a potential background for Germanium based neutrinoless double-beta decay search experiments such as GERDA or the LEGEND experiment. In this work we present a search for ^{77}Ge decays in the full GERDA Phase II data set. A delayed coincidence method was employed to identify the decay of ^{77}Ge via the isomeric state of ^{77}As ($9/2^+$, 475 keV, $T_{1/2} = 114 \mu\text{s}$, $^{77\text{m}}\text{As}$). New digital signal processing methods were employed to select and analyze pile-up signals. No signal was observed, and an upper limit on the production rate of ^{77}Ge was set at $< 0.216 \text{ nuc}/(\text{kg}\cdot\text{yr})$ (90% CL). This corresponds to a total production rate of ^{77}Ge and $^{77\text{m}}\text{Ge}$ of $< 0.38 \text{ nuc}/(\text{kg}\cdot\text{yr})$ (90% CL), assuming equal production rates. A previous Monte Carlo study predicted a value for in-situ ^{77}Ge and $^{77\text{m}}\text{Ge}$ production of $(0.21 \pm 0.07) \text{ nuc}/(\text{kg}\cdot\text{yr})$, a prediction that is now further corroborated by our experimental limit. Moreover, tagging the isomeric state of $^{77\text{m}}\text{As}$ can be utilised to further suppress the ^{77}Ge background. Considering the similar experimental configurations of LEGEND-1000 and GERDA, the cosmogenic background in LEGEND-1000 at LNGS is estimated to remain at a sub-dominant level.

1 Introduction

In-situ production of radioactive isotopes by atmospheric muons can represent a non-negligible background for experiments searching for rare events even when located deep underground. One such experiment is the GERDA (Germanium Detector Array) experiment [1] that searched for the neutrinoless double-beta ($0\nu\beta\beta$) decay in ^{76}Ge located underground below a rock overburden of about 3.5 km.w.e. at the LNGS (Laboratori Nazionali del Gran Sasso) of INFN.

In Phase II of the GERDA experiment, 40 (after upgrade 41) high-purity germanium (HPGe) detectors made from material isotopically enriched in ^{76}Ge were operated as bare crystals in a cryostat filled with 64 m³ liquid argon (LAr). The LAr served as both a coolant and an instrumented active shield. It allowed effective detection of the argon scintillation light produced by background events that deposit energy in the argon

surrounding the germanium detectors. The LAr cryostat was immersed in a 590 m³ water tank equipped with photomultipliers which, together with scintillator plates on top of the setup, served as a further shield against external radiation and as a muon veto system. In the event of a trigger in one of the HPGe detector channels, all HPGe readout channels were recorded for off-line analysis. $0\nu\beta\beta$ decay candidate events were required to have a point-like energy deposition in a single HPGe detector, and no signal in the liquid argon or the muon system. Based on these selection criteria, a quasi-background free search was performed with a total exposure in detector mass accumulated over Phase II of 103.7 kg·yr and, after combination with Phase I, a limit of on the half-life of $0\nu\beta\beta$ decay in ^{76}Ge was set to $T_{1/2} > 1.8 \times 10^{26}$ at 90% C.L. [2].

Previous simulations [3] identified the delayed decays of ^{77}Ge and its isomeric state $^{77\text{m}}\text{Ge}$, both produced by neutron capture on ^{76}Ge , as the dominant cosmogenic backgrounds in GERDA. The Q_β value of ^{77}Ge (2703 keV) and of the isomeric state are both above the $Q_{\beta\beta}$ value of ^{76}Ge (2039 keV). Thus, their β decays can deposit energy in the region of interest at $Q_{\beta\beta}$ and mimic a signal-like event. Conversely, ^{77}As , the decay product of ^{77}Ge , does not contribute to the background, since with $Q_\beta = 684 \text{ keV}$ it cannot contribute in the region of interest.

Recently, a $^{77(\text{m})}\text{Ge}^1$ production rate of $(0.21 \pm 0.01 \text{ (stat)} \pm 0.07 \text{ (sys)}) \text{ nuc}/(\text{kg}\cdot\text{yr})$ was obtained using a full GEANT4 simulation [4]. The systematic uncertainties were 35 %, dominated by muon-induced neutron production and propagation. At this rate, the $^{77(\text{m})}\text{Ge}$ background contribution at $Q_{\beta\beta}$ is estimated to be $\sim 10^{-5} \text{ cts}/(\text{keV}\cdot\text{kg}\cdot\text{yr})$ after applying the standard cuts used in GERDA. With the addition of a delayed coincidence cut as defined in the above paper, a background contribution of $(2.7 \pm 0.3) \times 10^{-6} \text{ cts}/(\text{keV}\cdot\text{kg}\cdot\text{yr})$ can be achieved. Using this as a proxy for the planned ^{76}Ge experiment LEGEND-1000 at LNGS this showed that the $^{77(\text{m})}\text{Ge}$ background contribution can be suppressed low enough to achieve a background at $Q_{\beta\beta}$ of $< 10^{-5} \text{ cts}/(\text{keV}\cdot\text{kg}\cdot\text{yr})$, which is a factor of 50 reduction with respect to GERDA [5]. Experimental validation of the predicted $^{77(\text{m})}\text{Ge}$ production rate and constraining uncertainties using GERDA data are therefore of paramount importance to consolidate the background model of LEGEND-1000.

This paper summarizes the present analysis to quantify the in-situ production of ^{77}Ge in its ground state ($T_{1/2} = 11.21 \text{ h}$ [7]) in GERDA by searching for its characteristic decay through the isomeric state ($9/2^+$, 475 keV, $T_{1/2} = 114 \mu\text{s}$) of its progeny ^{77}As . The anal-

¹The notation $^{77(\text{m})}\text{Ge}$ represents both ^{77}Ge and $^{77\text{m}}\text{Ge}$.

^acorrespondence: gerda-eb@mpi-hd.mpg.de

^bdeceased

^calso at: NRNU MEPhI, Moscow, Russia

^dpresent address: Duke University, Durham, NC USA

^ealso at: Moscow Inst. of Physics and Technology, Russia

^fpresent address: Semilab Zrt, Budapest, Hungary

^galso at: Dubna State University, Dubna, Russia

^hpermanent address: Nuclear Science Division, Berkeley, USA

ysis uses the full data set of the GERDA Phase II experiment with an exposure of 103.7 kg.yr. With the production rate estimate from above, this gives an expected number of about (22 ± 7) $^{77(\text{m})}\text{Ge}$ nuclei in either its ground state or isomeric state.

To isolate the ^{77}Ge decays, we search for a coincidence between the prompt β decay of ^{77}Ge and the delayed de-excitation of the isomeric $^{77\text{m}}\text{As}$ state. We require that the prompt energy deposition and the delayed de-excitation occur in the same detector. Figure 1 displays a simplified decay scheme of the ^{77}Ge - ^{77}As system. The time correlated signature of the beta decay into $^{77\text{m}}\text{As}$ and its delayed de-excitation leads to so-called pile-up signals in the GERDA data stream.

Special processing of the GERDA data was performed to isolate time-correlated candidates since they were discarded in the standard GERDA $0\nu\beta\beta$ decay analysis. Furthermore, new digital signal processing (DSP) routines were developed to extract the physical parameters of the pile-up signal. The DSP routines have been validated using generated data and the candidate event selection efficiencies and the uncertainties in the energy reconstruction were determined.

demonstrator experiment data [6]. Considering the larger overburden of the Sanford Underground Research Facility (SURF) at 4.3 km water equivalent (w.e.) compared to LNGS at 3.5 km w.e., the production rate of ^{77}Ge is expected to be lower in comparison. This analysis found no candidate event for this mechanism, but for other cosmogenic isotopes it found a factor of 2 agreement between simulation and data. However, due to the different shielding material, i.e. lead in MAJORANA and LAr in GERDA, it is difficult to use these results to validate the GERDA simulation, which further motivates the work presented in this paper.

We distinguish two classes of transitions: *prompt* transitions (β and subsequent prompt γ de-excitations), shown in Figure 1, start from the ground state of ^{77}Ge and end on the 475 keV ($T_{1/2} = 114\mu\text{s}$) isomeric state of $^{77\text{m}}\text{As}$. *Delayed* transitions, are those electromagnetic de-excitations that start from the 475 keV isomeric state and terminate at the ground state of ^{77}As . Since the half-life of $^{77\text{m}}\text{As}$ is longer than the charge collection time in GERDA’s HPGe detectors ($\lesssim 1.5\mu\text{s}$), the delayed transitions occur with sufficiently large time differences with respect to the prompt so that both transitions can be separated unambiguously in time. We call their combined occurrence in the same detector a *delayed coincidence*.

In Subsection 2.1 we identify the expected signature of the delayed coincidence in the GERDA experiment. Then, in Subsection 2.2 we present the DSP to reconstruct pile-up signals in the GERDA data and how we estimate their energies. Finally, in Subsection 2.3 we present the selection criteria to identify candidate delayed coincidences in the GERDA data and calculate the total selection efficiency.

In-situ cosmogenic interactions can produce both ^{77}Ge and $^{77\text{m}}\text{Ge}$. The isomeric state $^{77\text{m}}\text{Ge}$ undergoes an internal transition to the ground state ^{77}Ge with $(19 \pm 2)\%$. When $^{77\text{m}}\text{Ge}$ decays directly to ^{77}As , it has a 99 % probability of populating one of the four states that are energetically below the isomeric state $^{77\text{m}}\text{As}$. Therefore, $^{77\text{m}}\text{Ge}$ decays cannot be tagged through the $114\text{ }\mu\text{s}$ delayed coincidence. Conversely, $(33 \pm 1)\%$ of ^{77}Ge decays populate the isomeric state $^{77\text{m}}\text{As}$ (see Figure 1). About half of the prompt decays $((16 \pm 1)\%)$ that populate the isomeric state are direct transitions, while the other half come from consecutive gammas de-excitations from

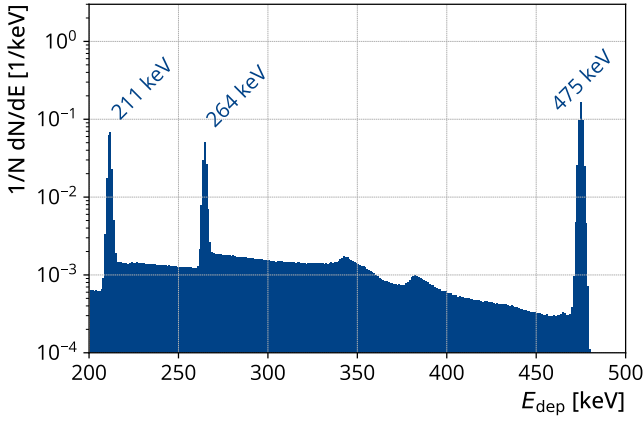


Fig. 2 Simulated energy distribution of the delayed gamma emission from the isomeric state in ^{77}As deposited in a HPGe. The peaks correspond to the full energy deposition of both gammas in the detector at 475 keV or the full energy deposition of only one of the gammas in the detector at 211 keV or 264 keV. The energy resolutions of each individual detector derived from the standard GERDA analysis were implemented.

higher levels of ^{77}As . The end-point energy of these decays into the isomeric state is 2228 keV (2703 keV – 475 keV). The rest of the beta decay branches (67 %) populate other states that miss the isomeric state in the consecutive gamma decay.

While the beta particle will deposit its energy in the germanium detector where the $^{77(\text{m})}\text{Ge}$ is produced, the gammas can also escape and deposit their energy in the liquid argon (LAr) or in other detectors. To simulate the prompt transitions of the ^{77}Ge decay into $^{77\text{m}}\text{As}$ in the GERDA Phase II experiment, we used the MaGe simulation framework [8]. We define the multiplicity as the total number of detectors with coincident energy deposition above 40 keV. At least one of these detectors must have an energy deposition above 200 keV. This additional condition avoids systematic uncertainties in modeling the online trigger threshold, which had different values during different data acquisition periods but was always set well below the above value. We find that > 75% of prompt transitions occur with a multiplicity of one, i.e., all energy is deposited in a single detector.

The delayed transitions were also simulated with MaGe. We found that 65 % of the energy is deposited only in the same detector as the prompt transition. Figure 2 shows the energy deposited in an HPGe of a delayed transition with multiplicity one. The spectrum shows full energy peaks at 211 keV, 264 keV, and at 475 keV due to the summation of the two gammas or the single gamma transition (see Figure 1).

GERDA used charge-sensitive preamplifiers with RC-feedback that shape the physical signal from a HPGe detector into a pulse consisting of a rapid change in output voltage followed by a slow exponential decay

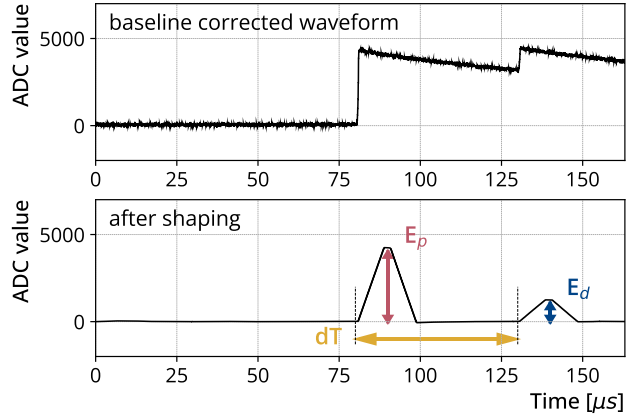


Fig. 3 An example of pile-up signal reconstruction. (Top) Example of a pile-up event waveform in the GERDA data stream. (Bottom) The waveform of the example pile-up event after applying a trapezoidal filter. The time difference between the signals is estimated by taking the difference between the triggers. Finally, the signal heights are extracted with a fixed time pick off.

($\tau \sim 150 \mu\text{s}$) back to the baseline. The time difference between the prompt and delayed transitions is of the same order as the decay constant of the charge sensitive amplifier. Therefore, in the previously mentioned most likely case where the delayed transition only deposits energy in the same detector, the signal produced by the delayed transition will appear as a pulse that lies on top of the pulse produced by the prompt transition also known as pile-up (e.g., see Figure 3, top).

An energy deposition in any of the 40(41) HPGe detectors generated a synchronous readout of the waveforms of all HPGe detectors. These coincident waveforms are referred to as one event. The length of the waveforms is $164 \mu\text{s}$, with the initial trigger centered at about $80 \mu\text{s}$. Therefore, a pile-up signal can occur either in the same waveform as the prompt signal (as see the example Figure 3) or in a waveform of a subsequent event. In the GERDA experiment, the data acquisition (DAQ) system is configured to record a new event if a trigger occurs more than $50 \mu\text{s}$ after the previous one, with the second waveform centered at $80 \mu\text{s}$. If the interval between two triggers is shorter than the full waveform duration ($164 \mu\text{s}$), the corresponding waveforms will overlap, meaning they share a common set of samples. Since the standard GERDA analysis rejects overlapping waveforms, we have implemented a new DSP tool to accurately reconstruct pile-up signals also for overlapping waveforms.

2.2 Pile-up signal reconstruction

The new DSP is based on the validated Majorana/GERDA Data Objects Library (MGDO), which are also used in the standard GERDA DSP [10]. The DSP transforms the original waveform with trapezoidal filters consisting of a pole-zero correction, a moving window differentiation, and a moving window average filter. A selection of filter lengths was chosen that are optimized for energy resolution and detection sensitivity. The filter length for a given pile-up signal is selected in steps according to the minimum time difference between the triggers. For example, for time differences $> 18 \mu\text{s}$, the moving window differentiation is $10 \mu\text{s}$ wide and the moving window average is $8 \mu\text{s}$, resulting in a total filter length of $18 \mu\text{s}$ and a flat top of $2 \mu\text{s}$. The time difference between signals in the same waveform is calculated as the difference between trigger positions. For pile-up signals in different events we extract the time difference using their timestamp in ns. The height of the signals are extracted with a fixed time pick-off at the 75 % point on the flat top. Figure 3 bottom shows an example of the DSP, extracting the peak heights and time difference between the signals. The DSP also extracts additional quality parameters from the waveforms such as a negative trigger to reject electromagnetic noise and non-physical pulses. We ran the new DSP on waveforms containing two pulses, extracting the heights of both the prompt and the delayed event, and on waveforms containing only the delayed pulse. For all other situations, we found that the original DSP gave similarly good results, and we used its energy estimation.

To calibrate the signal heights extracted from the waveform with the new DSP, we use the waveforms of signals with already estimated energies from the standard GERDA analysis. We apply the same trapezoidal filter to 50 consecutive single signal waveforms after the delayed coincidence candidate in the same detector. We plot their signal height against their previously estimated energy, associate them with an uncertainty corresponding to the resolution of the detector at that energy and extract the calibration by fitting the plot with a linear function. This gives us the calibrated reconstructed prompt (E_p) and delayed (E_d) energies.

Since this is a non-standard approach to energy calibration, we performed several cross-checks. In GERDA, to obtain a calibration, dedicated calibration runs were performed before and after each physics run [11]. During those, three ^{228}Th sources were automatically lowered into the LAr cryostat in close proximity to the HPGe detectors. The calibration data are populated with a large contribution of pile-ups from the gammas emitted by the progeny ^{208}Tl . Since these signals

are not correlated, they are called first and second instead of prompt and delayed pulse. Figure 4 shows the energy distribution of the first and second pulse energies of pile-up signals in the calibration data, where the two signals are contained in the waveform of one event. We can reconstruct the expected gamma lines for both pulses in a pile-up signal. The energy distribution of the first pulse shows energy resolutions of e.g. a Full Width Half Maximum (FWHM) of 4.2 keV at 2.6 MeV. Compared to the exposure weighted resolution in the standard GERDA analysis of about 3.7 keV at 2.6 MeV this value is slightly higher. In contrast to the standard GERDA analysis, the DSP parameters in this study were optimized for pile-up recognition rather than for achieving optimal energy resolution. The energy distribution of the second pulse exhibits a significant degradation in resolution. For instance, a FWHM of 8.4 keV at 2.6 MeV is roughly twice that of the first pulse. This degradation arises because the second pulse occurs on the falling tail of the first pulse, resulting in suboptimal baseline reconstruction. In addition, the gamma lines exhibit low-energy tailing and a slight energy shift of approximately -1 keV at 2.6 MeV, here referred to as the energy bias (see Fig. 4).

To further investigate the energy resolution and bias of individual candidates delayed coincidences, we generated data with similar signatures. We chose single pulse waveforms from the calibration data with similar prompt energy to the candidate prompt pulse. Then we selected another single pulse waveform with energies near the ^{208}Tl gamma lines as the delayed pulse and added them with a time difference similar to the candidate delayed coincidences. Subsequently, we reconstructed the energy of the generated pile-up signal with the DSP and extracted the energy resolution and bias from the reconstructed gamma lines by fitting the peaks with a Gaussian peak, a linear background, a step function, and a tail function similar to [11]. We also modeled the energy resolution in a similar way by taking the square root of a linear function and fitting it to the peaks full-width-at-tenth-maximum (FWTM). To obtain the energy resolution of the candidate pile-up signal, we interpolated this model at the reconstructed delayed energy. We defined the bias of the candidate pile-up signal energy as the largest difference between the reconstructed peak mean energy and the expected energy of all gamma lines. We found that the bias is the largest for delayed coincidences with short time differences but usually well below 1 keV. With this we estimated a FWTM and bias range for each candidate delayed coincidence.

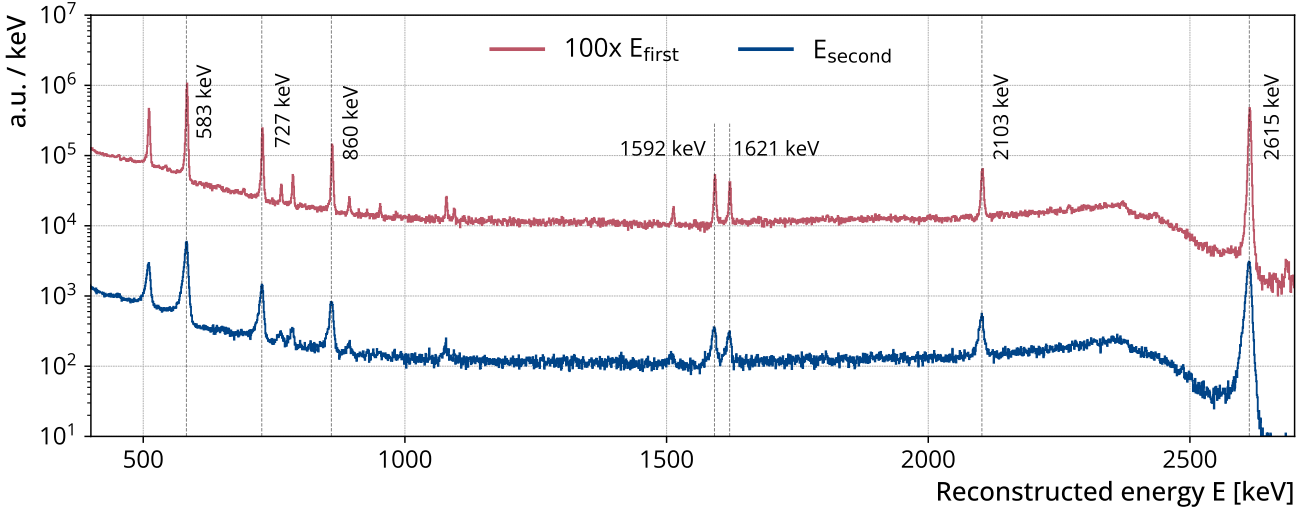


Fig. 4 Reconstructed energy spectra for the first and second pulse in a pile-up signal in the calibration data where two signals are contained in the waveform of one event. The red histogram corresponds to the first pulses energies, while the blue histogram corresponds to the second pulses energies. The former distribution was scaled by a factor of 100 to illustrate the differences between the spectra. Both spectra reconstruct the expected ^{208}Tl gamma lines well. The spectra of the second pulses consistently shows larger resolution and a slight tail to lower energies.

2.3 Candidate selection

Based on the simulation results, we define the selection criteria for the prompt and delayed energy and the multiplicity as well as the time difference of the candidates.

We define a selection condition for prompt transition candidates by requiring that they have (i) a multiplicity of one and (ii) an energy E_p between 200 keV and 2228 keV equal to the maximum total deposited energy. The simulation shows that 74.6 % of prompt transitions satisfy these conditions.

We further define a delayed transition selection condition that candidate delayed transitions must (i) have multiplicity one, (ii) occur in the same detector as the prompt transition, and (iii) have one of the three gamma energies (211 keV, 264 keV or 475 keV) lie within the respective reconstructed energy acceptance region E_d defined by the FWTM range plus bias. We chose to use the FWTM (containing 96 % of the peak area) rather than the FWHM to account for possible tails as gamma lines in the energy spectrum of the delayed candidate signals may deviate from the expected Gaussian distribution (see Figure 4). To account for a potential bias in the reconstructed delayed energies, we extend the acceptance region of an individual delayed coincidence candidate asymmetrically by the minimum and maximum bias described in Subsection 2.2. We find that 46.2 % of the delayed transitions satisfy the above conditions. The energy and multiplicity selection efficiency of 34.5 % in Table 1 is the combined efficiency to select

both the prompt and the delayed transition with these conditions.

Finally, we require that the time difference dT between a prompt and a delayed transition candidate be no greater than five times the lifetime of the isomeric state ($822 \mu\text{s}$). The corresponding time difference selection efficiency is also given in Table 1.

We now define the criteria for selecting the candidates based on the quality parameters extracted from the standard GERDA analysis as well as the pile-up reconstruction using our DSP. Due to the difference in signature between delayed coincidences with signals in the same or different waveforms, we define three different regions depending on the time difference between the signals.

1. For time differences less than $70 \mu\text{s}$, the two signals will be contained in one waveform. This is because the first signal is approximately in the center at $80 \mu\text{s}$ of the long $164 \mu\text{s}$ waveform. We require that the quality parameters that are extracted from the new DSP satisfy a set of conditions. A candidate for a delayed coincidence with corresponding time differences must have (i) exactly two triggers and (ii) pass through the additional quality parameter cuts.

2. For time differences between $70 \mu\text{s}$ and $164 \mu\text{s}$, the two signals are contained in separate events, but are still so close together that their waveforms overlap. Since the DAQ records a new event when a trigger occurs at least $50 \mu\text{s}$ after the previous one, we are sensitive to all signals in that time range. In the standard GERDA analysis, the second event was discarded before

the DSP step. This is due to a short busy period of the DAQ of the order of 100 ns during the saving process of the first event, which interrupted the recording of the waveform of the following event. We reconstructed such waveforms by interpolating in these periods. Since these events were not processed in the standard GERDA analysis, we applied DSP to all its waveforms. Using the extracted quality parameters, we require that a candidate delayed signal waveform with corresponding time difference (i) contains only one trigger and (ii) pass through the additional quality parameter cuts.

3. For time differences above 164 μs , the waveforms of the two events no longer overlap, and both events have been processed in the standard GERDA analysis. We use the standard GERDA quality conditions to differentiate signal candidates from non-physical signals. We require that the prompt waveform satisfy all standard GERDA quality conditions, while the delayed waveform satisfies a subset of these conditions consistent with a signal on an exponential tail. For these events, we did not apply the new DSP to either the prompt or the delayed waveform because the standard GERDA analysis already provided reliable values of the prompt and delayed energies.

To estimate the resulting pile-up signal selection efficiency, we generated pile-up signals with energies in the corresponding energy ranges and time differences sampled from an exponential distribution according to the lifetime of $^{77\text{m}}\text{As}$. We define the pile-up signal selection efficiency as the number of signals that pass the entire pile-up signal selection procedure over the total amount generated. The final pile-up signal selection efficiency is given in Table 1. We tested whether the pile-up signal selection efficiency depends on certain parameters. Figure 5 shows the pile-up signal selection efficiency plotted over the time difference range up to 20 μs . It shows a jump from zero to almost one at 4.5 μs , which shows that our analysis is sensitive to pile-ups with time differences above this threshold. The efficiency of pile-up signal selection remains constant above 20 μs up to the upper limit of time difference selection at $5\tau_{77\text{mAs}} = 822\mu\text{s}$. Therefore, the only dead time in our analysis is due to the delayed signals that occur at time differences smaller than 4.5 μs . We also tested for a prompt or delayed energy dependence and found it to be constant over the ranges of interest.

The total selection efficiency $\epsilon_{\text{total}} = \epsilon_{\text{em}} \times \epsilon_{\text{dT}} \times \epsilon_{\text{pile-up}}$ amounts to 32.4%.

3 Result

We applied the pile-up signal selection to the entire GERDA Phase II data set, which has an exposure of

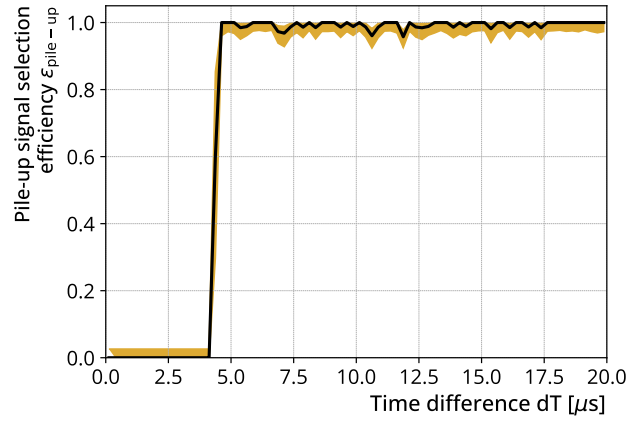


Fig. 5 Pile-up signal selection efficiency plotted over the time difference between generated pile-up signals. Our new DSP is sensitive for delayed coincidences starting at time differences $> 4.5\mu\text{s}$. Individual events in this range were rejected due to quality cuts. Black: central value. Yellow: 68% uncertainty band.

Table 1 Delayed coincidence selection efficiencies. The uncertainty of these values is in the order of $< 0.5\%$.

Energy and multiplicity selection efficiency ϵ_{em}	34.5%
prompt contribution $\epsilon_{\text{em}}^{\text{p}}$	74.6%
delayed contribution $\epsilon_{\text{em}}^{\text{d}}$	46.2%
Time difference selection efficiency ϵ_{dT}	99.3%
Pile-up signal selection efficiency $\epsilon_{\text{pile-up}}$	94.9%
Total selection efficiency ϵ_{total}	32.4%

103.7 kg \cdot yr. Figure 6 shows a scatter plot of the delayed coincidence candidates that pass all the selection criteria of the previous section apart from the delayed energy selection. The black dots represent the reconstructed values of delayed energy and time difference, while the colored bars in x-direction represent the delayed energy FWTM plus bias acceptance region (linearly summed) estimated individually for each candidate. A candidate is accepted if its reconstructed delayed energy acceptance region overlaps with one of the expected gamma energies. We find that there is no candidate delayed coincidence that passes this selection ($N_{\text{obs}} = 0$ cts).

Random coincidences are the only known background source in this analysis. Using the average signal rates in each detector for the 1 FWTM energy ranges around the gamma lines, we calculated the number of expected random coincidence signals considering our selection criteria to be $N_{\text{rc}} = 0.04$ cts.

For a wider range of delayed energies between 200 keV and 500 keV the expected number of random coincidence signals is 0.2 cts compared to eight delayed coincidence candidates observed (see Figure 6). The time and energy distributions of these signals differ significantly from the expected ^{77}Ge delayed coincidence time and

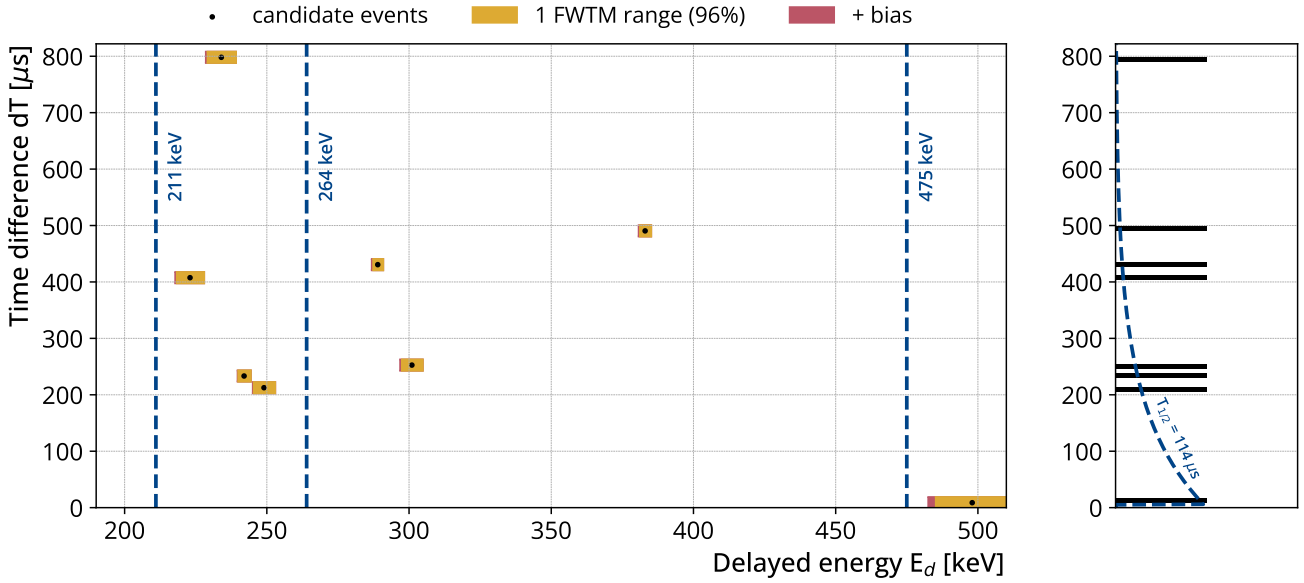


Fig. 6 The distribution of all 8 candidate delayed coincidences after the multiplicity condition plotted dT over E_d . The energy windows around the points correspond to the linear combination of the full-width-at-tenth-maximum (FWTM) window (yellow) plus the asymmetric bias window (red). The FWTM window covers about 97% of the gamma peak area. The vertical size of the data is enlarged for better visualization. The blue lines correspond to the gamma energies of the internal transitions from ^{77m}As . A delayed coincidence candidate is rejected, if its energy window misses any of the three gamma lines. We found no candidate delayed coincidence that satisfies this condition resulting in $N_{\text{obs}} = 0$ cts. The right part shows a projection of the candidates onto dT . The blue line corresponds to the expected distribution for ^{77m}As delayed coincidences.

energy distributions, and thus can be excluded as a majority contributor to these events. If we ignore the time distribution, for the ^{77}Ge delayed coincidences that deposit energy above 200 keV, the fraction of energy depositions in the continuum region is around 26 %, with the rest in the peaks. Without an event in the peaks, it is therefore feasible that one or two events in the continuum could be ^{77}Ge delayed coincidences, but more would be unlikely. A search for other sources generating delayed coincidences such as delayed neutron capture in muon-induced showers, ^{214}Bi - ^{214}Po decays, or delayed de-excitation in other isotopes, was performed but was inconclusive.

With $N_{\text{obs}} = 0$ cts and $N_{\text{rc}} = 0.04$ cts, we can determine an upper limit of < 2.4 cts (90% CL) on the number of delayed coincidences by applying Feldman-Cousins method [12]. We can convert the number of delayed coincidences to the number of ^{77}Ge decays by dividing it with the product of the total selection efficiency and the ratio of delayed coincidences per ^{77}Ge decay ($(33 \pm 1)\%$, see Figure 1). We treat the uncertainty by integrating over the nuisance parameter as described in [13,14]. We found an upper limit on the number of ^{77}Ge decays of $N_{77\text{Ge}} = 22.4$ decays (90% CL).

Considering that the ^{77}Ge has a half-life much shorter than the time during which GERDA Phase II acquired

the 103.7 kg·yr exposure, any ^{77}Ge must have been produced in-situ. We can therefore calculate an upper limit on the ^{77}Ge production rate of < 0.216 nuc/(kg · yr) (90% CL).

The ^{77}Ge in GERDA is mainly produced by cosmogenic activation. Radiogenic neutrons from natural decay chains originating outside the experiment are absorbed by the water tank and cannot reach the HPGe detectors. In the LAr cryostat, a cosmic muon can produce particle showers with high neutron multiplicity. The vast majority of neutrons are captured by ^{40}Ar or by the water in the water tank. A minority is captured by ^{76}Ge , producing either the ground state ^{77}Ge or the isomeric state ^{77m}Ge . The production ratio between the two depends on the kinetic energy of the neutron when absorbed. Following the arguments from our previous work [4] and corroborated by statistical model calculations [15], we assign a probability for the direct ground state population of $\epsilon_d = (50 \pm 10)\%$. In addition, the probability of the internal transition from the isomeric state into the ground state of $\epsilon_{\text{IT}} = (19 \pm 2)\%$ has to be taken into account. Therefore, the probability to populate the ground state ϵ_g after neutron capture is

$$\epsilon_g = (\epsilon_d + (1 - \epsilon_d) \cdot \epsilon_{\text{IT}}) = (59.5 \pm 8.1)\%.$$

Assuming that all delayed coincidences are of cosmogenic origin, we can use ϵ_g to calculate the sum of the ^{77}Ge and ^{77m}Ge production rate. We treat the nuisance

parameters as before. Applying the Feldman-Cousins method, we get a total $^{77(\text{m})}\text{Ge}$ production rate of

$$< 0.38 \text{ nuc}/(\text{kg}\cdot\text{yr}) \text{ (90\% CL)}.$$

This is the strongest experimental constraint on the $^{77(\text{m})}\text{Ge}$ production rate at LNGS and is about a factor of two larger than the MC prediction of $(0.21 \pm 0.01(\text{stat}) \pm 0.07(\text{sys})) \text{ nuc}/(\text{kg}\cdot\text{yr})$. For completeness, we refer here to a previous analysis performed on the GERDA data, in which an upper limit of $< 4.1 \text{ nuc}/(\text{kg}\cdot\text{yr})$ (90% CL) was derived in [16].

With our constraint on the $^{77(\text{m})}\text{Ge}$ production rate, we can update the predictions from previous simulations [4]. To this end, the simulated production rate estimate is treated as a prior with a Gaussian distribution centered at $0.21 \text{ nuc}/(\text{kg}\cdot\text{yr})$ and an uncertainty of $0.07 \text{ nuc}/(\text{kg}\cdot\text{yr})$ (1σ). Our constraint on the $^{77(\text{m})}\text{Ge}$ production rate is modeled by an exponential function as illustrated in Fig. 7. The posterior has a central value of $0.18 \text{ nuc}/(\text{kg}\cdot\text{yr})$ with a 1σ credibility interval of $[0.106, 0.251] \text{ nuc}/(\text{kg}\cdot\text{yr})$. Relatively, the posterior predicts the simulated production rate scales by a factor of $0.85^{+0.35}_{-0.34}$ compared to the original estimate.

Previous simulations of the background from $^{77(\text{m})}\text{Ge}$ decays in GERDA predicted a background index (BI) of $(2.7 \pm 0.3) \times 10^{-6} \text{ cts}/(\text{keV}\cdot\text{kg}\cdot\text{yr})$ with individual contributions of $(1.2 \pm 0.5) \times 10^{-6} \text{ cts}/(\text{keV}\cdot\text{kg}\cdot\text{yr})$ and $(1.5 \pm 0.2) \times 10^{-6} \text{ cts}/(\text{keV}\cdot\text{kg}\cdot\text{yr})$ from $^{77\text{m}}\text{Ge}$ and ^{77}Ge respectively excluding the previously mentioned systematic uncertainties of 35% [4]. This BI is achieved after active background suppression (i.e. detector anti-coincidence, rejection by liquid argon anti-coincidence and pulse shape discrimination (PSD)), and after applying a veto condition after tagged muons. Applying the scaling factor for the $^{77(\text{m})}\text{Ge}$ production rate, we estimate a contribution to BI of $(2.3 \pm 0.1(\text{stat}) \pm 1.0(\text{sys})) \times 10^{-6} \text{ cts}/(\text{keV}\cdot\text{kg}\cdot\text{yr})$. The statistical uncertainty is due to the finite exposure simulated in the previous simulation study. The systematic uncertainty consists of the approximately symmetric distribution of the production rate scaling factor with standard deviation 35% and the uncertainty of the direct population of the ground state after production of 10%.

Tagging the delayed coincidence decay through the isomeric state in ^{77}As can not only be used to estimate the production rate, but also to tag and reject ^{77}Ge decays in the $0\nu\beta\beta$ decay search. To estimate how many such ^{77}Ge decays can be additionally rejected, we simulated ^{77}Ge decays using a MaGe simulation of the GERDA setup to and modeled the active background suppression in the same way as in [4]. We found that of the ^{77}Ge decays with an energy around $Q_{\beta\beta}$, 92% are rejected by the active background suppression. Of the

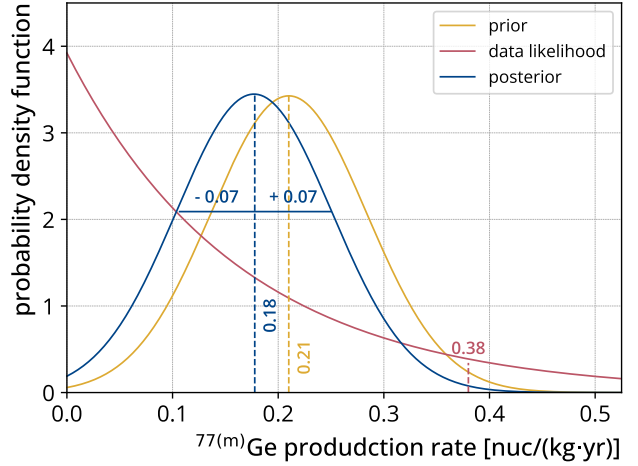


Fig. 7 Bayesian update of the simulated production rate using the likelihood of the GERDA data estimated in this analysis.

surviving events, about $(62 \pm 1)\%$ produce a delayed coincidence signal with $E_d > 200 \text{ keV}$ and $dT > 10 \mu\text{s}$. The large contribution of such events can be explained by the fact that 16% of ^{77}Ge decay directly into the isomeric state, which are simple beta decays with a similar topology to $0\nu\beta\beta$ decays and therefore predominantly survive the analysis cuts. By rejecting events with the delayed coincidence signal mentioned above, we estimate that a $^{77(\text{m})}\text{Ge}$ background index contribution of $(1.50 \pm 0.07(\text{stat}) \pm 0.67(\text{sys})) \times 10^{-6} \text{ cts}/(\text{keV}\cdot\text{kg}\cdot\text{yr})$ is achievable. The contribution of this rejection to the $0\nu\beta\beta$ decay survival fraction is negligible due to the low random coincidence rate.

4 Implications and Conclusions

LEGEND is the successor experiment to GERDA, which in its first phase, LEGEND-200, reuses the GERDA cryostat at LNGS and operates up to 200 kg of HPGe detectors enriched in the isotope ^{76}Ge . In the second phase, LEGEND-1000, one tonne of enriched HPGe detectors will be deployed in a new experimental infrastructure in Hall C of LNGS. After one year of LEGEND-200 data taking with the final detector mass, the sensitivity of the analysis presented here will double, tightening the constraint on the $^{77(\text{m})}\text{Ge}$ production rate by a factor of two, or potentially revealing a signal.

A previous simulation for LEGEND-1000, also based on GEANT4, gave a $^{77(\text{m})}\text{Ge}$ production rate of $(0.33 \pm 0.01(\text{stat}) \pm 0.12(\text{sys})) \text{ nuc}/(\text{kg}\cdot\text{yr})$ [17]. The approximately 1.6-fold increase in the $^{77(\text{m})}\text{Ge}$ production rate is attributed to the larger LAr volume compared to GERDA, which results in a higher neutron flux at the HPGe detectors and consequently a greater neutron capture

rate. As described in [17], a neutron moderator will be installed around the HPGe strings, dividing the liquid argon (LAr) volume into an inner and an outer region. This design aims to moderate neutrons crossing from the outer to the inner region to lower energies where capture on ^{40}Ar is more likely than on ^{76}Ge . By thus removing the contribution of neutrons originating outside the moderator, the $^{77\text{m}}\text{Ge}$ production rate is effectively reduced to a level below that observed in GERDA. As this decouples the production rate from the size of the cryostat, changes in the ongoing development of the experiment geometry are not expected to change this estimate. Furthermore, study [17] estimates that only 2.3% of all $^{77\text{m}}\text{Ge}$ decays in LEGEND-1000 will survive the veto condition following tagged muons. This 2.6-fold reduction in the survival fraction, compared to the 6% observed in GERDA [4], is primarily attributed to the tagging of neutrons in liquid argon in hadronic showers, which exhibit high neutron multiplicity. Combined with the tagging of the ^{77}Ge decays transitioning through the isomeric state in ^{77}As , we estimate that the in-situ cosmogenic background contribution for LEGEND-1000 will be below 10^{-6} cts/(keV.kg.yr).² The goal of LEGEND-1000 is to achieve a background index of $< 10^{-5}$ cts/(keV.kg.yr) for a quasi-background-free search for $0\nu\beta\beta$ decays [5]. The contribution of in-situ cosmogenic background thus accounts for $\leq 10\%$ of the total background budget. These findings indicate that the rock overburden at LNGS, combined with the suppression strategies discussed in [4, 17], and the delayed coincidence method to identify ^{77}Ge decay via the isomeric state of ^{77}As presented in this paper, are highly effective in reducing the cosmogenic background in LEGEND-1000 to a sub-dominant level.

Acknowledgements The GERDA experiment is supported financially by the German Federal Ministry for Education and

²This estimate is based on the background estimates of GERDA for $^{77\text{m}}\text{Ge}$ of $(1.2 \pm 0.5) \times 10^{-6}$ cts/(keV.kg.yr), and for ^{77}Ge of $(1.5 \pm 0.2) \times 10^{-6}$ cts/(keV.kg.yr), and the survival fractions for the additional cuts (survival fraction of ^{77}Ge after $^{77\text{m}}\text{As}$ decay tagging: $(1 - 62\%) = 38\%$; survival fraction of $^{77\text{m}}\text{Ge}$ after muon tagging: 2.3% (6%) in LEGEND-1000 (GERDA) after scaling by the Bayesian update of the simulation estimate (0.85).

$$8.8 \times 10^{-7} \text{ cts/(keV.kg.yr)} = \\ 0.85 \times [1.5 \times 10^{-6} \text{ cts/(keV.kg.yr)} \times 38\% + \\ 1.2 \times 10^{-6} \text{ cts/(keV.kg.yr)} \times (2.3\%/6\%)].$$

Since the background contribution of $^{77\text{m}}\text{Ge}$ in GERDA already accounted for the survival fraction, the corresponding LEGEND-1000 estimate was scaled according to the better survival fraction. In addition, the background index contribution is expected to be lower in LEGEND-1000 compared to GERDA, as the neutron moderator will reduce the production rate of cosmogenic isotopes. These estimates can also be refined by use of the results from [15].

Research (BMBF), the German Research Foundation (DFG), the Italian Istituto Nazionale di Fisica Nucleare (INFN), the Max Planck Society (MPG), the Polish National Science Centre (NCN, Grant number UMO-2020/37/B/ST2/03905), the Polish Ministry of Science and Higher Education (MNiSW, Grant number DIR/WK/2018/08), the Russian Foundation for Basic Research, and the Swiss National Science Foundation (SNF). This project has received funding/support from the European Union's Horizon 2020 research and innovation programme under the Marie Skłodowska-Curie Grant agreements no 690575 and no 674896. This work was supported by the Science and Technology Facilities Council, part of the UK Research and Innovation (Grant no. ST/T004169/1). The institutions acknowledge also internal financial support. The GERDA collaboration thanks the directors and the staff of the LNGS for their continuous strong support of the GERDA experiment.

References

1. M. Agostini *et al.* (GERDA Collab.), Upgrade for Phase II of the GERDA experiment, *Eur. Phys. J. C* 78, 388 (2018) <https://doi.org/10.1140/epjc/s10052-018-5812-2>
2. M. Agostini *et al.* (GERDA Collab.), Final Results of GERDA on the Search for Neutrinoless Double- β Decay, *Phys. Rev. Lett.* 125, 252502 (2020) <https://doi.org/10.1103/PhysRevLett.125.252502>
3. L. Pandola *et al.*, Monte Carlo evaluation of the muon-induced background in the GERDA double beta decay experiment, *Nucl. Instrum. Methods A* 570, 149–158 (2007) <https://doi.org/10.1016/j.nima.2006.10.103>
4. C. Wiesinger, L. Pandola and S. Schönert, Virtual depth by active background suppression: Revisiting the cosmic muon induced background of GERDA Phase II, *Eur. Phys. J. C* 78, 597 (2018) <https://doi.org/10.1140/epjc/s10052-018-6079-3>
5. N. Abgrall *et al.* (LEGEND Collab.), The Large Enriched Germanium Experiment for Neutrinoless $\beta\beta$ Decay: LEGEND-1000 Preconceptual Design Report, arXiv (2021) <https://doi.org/10.48550/arXiv.2107.11462>
6. I. J. Arnuist *et al.*, (MAJORANA Collab.), Signatures of muonic activation in the MAJORANA Demonstrator, *Phys. Rev. C* 105, 014617 (2022) <https://doi.org/10.1103/PhysRevC.105.014617>
7. From ENSDF database as of February 21st, 2024. Version available at <http://www.nndc.bnl.gov/ensarchivals/FullEvaluationBalrajSinghENSDF30-Sep-2020>
8. M. Boswell *et al.*, MaGe – a Geant4-based Monte Carlo application framework for low-background germanium experiments. *IEEE Trans. Nucl. Sci.* 58, 1212 (2011) <https://doi.org/10.1109/TNS.2011.2144619>
9. A. Lazzaro, Signal processing and event classification for a background free neutrinoless double beta decay search with the GERDA experiment, PhD Thesis, Technische Universität München (2019) <https://mediatum.ub.tum.de/1507626>
10. M. Agostini *et al.*, The MGDO software library for data analysis in Ge neutrinoless double-beta decay experiments, *J. Phys. Conf. Ser.* 375 042027 (2012) <https://doi.org/10.1088/1742-6596/375/1/042027>
11. M. Agostini *et al.* (GERDA Collab.), Calibration of the GERDA experiment, *Eur. J. Phys. C* 81 (2021) 682 <https://doi.org/10.1140/epjc/s10052-021-09403-2>
12. G. J. Feldman and R. D. Cousins, A Unified approach to the classical statistical analysis of small signals, *Phys. Rev. D* 57 (1998) 3873–3889 <https://doi.org/10.1103/PhysRevD.57.3873>

-
13. R. D. Cousins and V. Highland, Incorporating systematic uncertainties into an upper limit, Nucl. Instrum. Meth. A 320 (1992) 331-33 [https://doi.org/10.1016/0168-9002\(92\)90794-5](https://doi.org/10.1016/0168-9002(92)90794-5)
 14. R. L. Workman *et al.* (Particle Data Group), Prog. Theor. Exp. Phys. 2022, 083C01 (2022)
 15. P. Grabmayr, Cross sections and gamma cascades in ^{77}Ge needed for background reduction in $0\nu\beta\beta$ experiments on ^{76}Ge , Eur. Phys. J. A (2024) 60, 115, <https://doi.org/10.1140/epja/s10050-024-01336-0>
 16. L. Vanhoefer, Limitations of Rare Event HPGe Experiments due to Muon-Induced Neutron Background, PhD Thesis, Technische Universität München (2018) <https://mediatum.ub.tum.de/1446626>
 17. M. Neuberger, M. Morella *et al.*, Strategies for cosmogenic $^{77(\text{m})}\text{Ge}$ reduction for LEGEND-1000 Experiment, Poster, Neutrino 2022 <https://doi.org/10.5281/zenodo.6804443>